THERMAL EMISSION SPECTRAL CHARACTERIZATION OF SANDSTONES AND MUDSTONES. M. T. Thorpe[1], A. D. Rogers[1] and T. Bristow [2], [1]Stony Brook University, Stony Brook, NY 117794-2100, michael.thorpe@stonybrook.edu, [2]NASA Ames Research Center, Moffett Field, Mountain View, CA 94035, thomas.f.bristow@nasa.gov

Introduction: Numerous observations from orbital and landed missions suggest that some Martian terrains have a rich sedimentary history that was shaped as result of aqueous activity [e.g. 1-2]. Given that the mineralogy is a key aspect in understanding chemical and physical conditions of sedimentary transport, deposition, and provenance, the expansion of remote sensing capability in determining rock composition becomes critically important. The opportunity to enhance the understanding of sedimentary rock thermal emission features is therefore key in future Mars research.

Laboratory techniques developed by [3], established a foundation for constructing a thermal emission spectral library of common rock-forming minerals [4]. Using these spectral libraries, mineral abundances were able to be determined from the mathematical unmixing of bulk rock spectra using linear least squares techniques [5]. Subsequent studies focused on bulk rock spectral characterization of igneous and metamorphic rocks [6], ultramafic rocks [7], basalts and andesites [8], weathered granites [9], evaporites [10], and a limited set of mudstones [11]. The overall conclusion from these studies recognized thermal emission spectroscopy as a valid technique, within ~ ±15%, for bulk rock mineral abundances. However, generally, there is a knowledge gap that still exists regarding the spectral behavior of sedimentary rocks, which can have varying grain size, porosity, and composition. For fine-grained materials, model accuracy might be expected to worsen due to optical transparency of thin grains. To that end, we assess the accuracy of mineral abundance determinations from thermal emission spectral models from a suite of mudstones and sandstones.

Methods: For this work, 12 sandstones and 5 mudstones were examined using a cross analytical approach consisting of thermal emission spectroscopy, Raman micro-imaging spectroscopy, quantitative X-ray diffraction, and traditional optical point counts. Thermal emission spectra were collected at the Stony Brook University Vibrational Spectroscopy Laboratory over a spectral range of 4000-200 cm^{-1} (2.5-50 μm) at a resolution of 4 cm^{-1}. The emissivity spectra of individual rock samples were modeled with mineral spectra using a nonnegative least squares method [12]. A modified spectral library constructed from the Arizona State University (ASU) database was used in the models and consisted of 129 mineral spectra collected from sand-sized or larger particles, or, for the case of clays, pressed pellets. Raman micro-imaging spectroscopy was also completed at Stony Brook University under a 50 X optical magnification. Individual Raman spectra were collected at each pixel within a 175 x 175 μm grid resulting in 30,625 single point spectra. Powdered X-ray diffraction (XRD) was completed using a Rigaku SmartLab Automatic X-ray Diffractometer system located at NASA's Ames Research Center in Moffett Field. Full pattern fitting techniques were employed to derive mineral abundances. Traditional point counts were conducted by systematically scanning the thin section and optically identifying ~ 250 points.

Results: Thermal emission spectra of sandstones and mudstones display absorptions that are characteristic of component crystal structures that can be generalized based on wavelength position and shape (Fig. 1). Modal mineralogy determined from petrologic point counts (known) are compared with spectrally derived (modeled) abundances for each sandstone (Fig 2.), whereas XRD abundances serve as the known for mudstone comparisons (Fig. 3). Linear comparison between total quartz, total feldspar, and the sum of all other mineral abundances test the accuracy of TIR unmixing models. The "other" class includes what is interpreted as the matrix (~ < 30μm) component, in this case mainly clays. This generalization for TIR mineral abundances may inherently result in incorrect estimation of mineral phases, because the matrix may also include quartz and feldspar. However, for the sake of comparison, it serves as a valuable assumption to assess bulk mineralogy results.

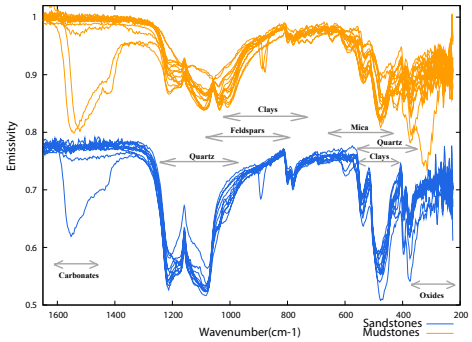

Figure 1. TIR spectra of sandstones and mudstones with generalized mineral group contributions

For sandstones, quartz displays the lowest mean difference, which coincides with the almost perfect linear fit (Table 1). Both feldspar and "other" also display strong correlations but with slightly higher average differences. These sandstone absolute differences and uncertainties fall within the accuracy associated

with traditional point counting techniques, which also compares well with previously mentioned bulk rock TIR models.

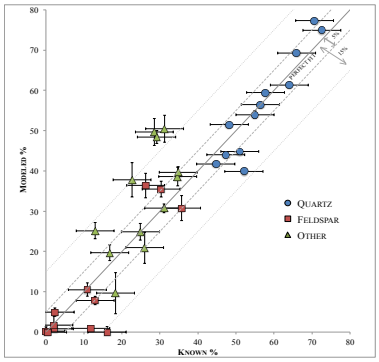

Figure 2. Sandstone point counts (known) vs. TIR models

In comparison, for mudstones, feldspar displays the lowest average absolute difference between the measured and modeled abundances (Table 1). Where as quartz and the "other" exhibit slightly higher mean differences.

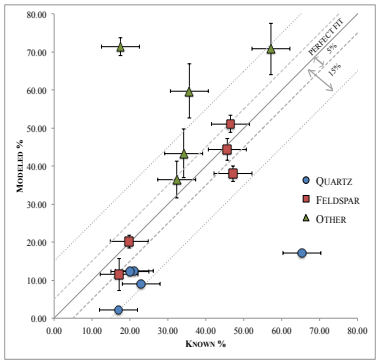

Figure 3. Mudstone XRD abundances (known) vs. TIR models

Discussion: Common sandstone composition (as determined by traditional point counts) consisted of quartz, feldspars, micas, clays, and a matrix/cement component unique to each sample; whereas, mudstone composition (as determined by XRD and microRaman) typically was comprised of quartz, plagioclase, and an abundant amount of a clay sized multi-component mineral mixture. Derived mineralogy from TIR spectra are highly correlated with these results; however, larger mineral clasts display a more conservative linear mixing behavior in comparison to mineral phases that make up the more fine-grained matrix component. For the 5 mudstones studied thus far, mineral groups with the largest discrepancy are sheet silicates and carbonates. Sheet silicates are commonly modeled at much lower abundances than indicated by the XRD analysis; however, the TIR models do include a significant abundance of glass. Because glass phases and poorly crystalline silicates or amorphous phases are spectrally similar in the TIR, this may explain the inconsistency. Conversely, for one sample, carbonates are modeled in significant abundance (> 40%) in the TIR, but not at all in the XRD analysis. Carbonates are clearly present in the sample, demonstrated by a strong absorption near 1550 cm $^{-1}$. These discrepancies will be analyzed further in the future.

Table 1. SS: Sandstone MS: Mudstone	**SS Mean ± 1 σ Diff (%)**	**MS Mean ± 1 σ Diff (%)**	**SS Median Diff (%)**	**MS Median Diff (%)**
Quartz	3.8 ± 3.2	18.7 ± 13.9	3.1	6.6
Feldspar	4.8 ± 5.1	4.2 ± 4.2	3.7	3.6
Other	9.4 ± 7.2	21.0 ± 13.6	6.8	19.8

The mineralogical results of this work provide TIR bulk rock abundances that are within 10 vol % for sandstones and within 20 vol % for mudstones, in comparison to the other techniques investigated. The identification of mineral phases that contribute to the < 30 μm grain size fraction remains highly ambiguous among the techniques examined, with each technique constrained by its own intrinsic limitations. Traditional petrographic analysis of thin sections produces accurate estimates of mineral clasts but can only qualitatively assess the content in the matrix fraction. Micro-Raman analysis is limited by highly fluorescent phases, small sampling areas, and also the present lack of laboratory work demonstrating linear contributions in multi-component spectra. X-ray diffraction requires extended sample preparation in order to identify non-crystalline (or poorly crystalline) phases that may be present in the matrix. TIR spectral modeling is affected by fine-grained, intimate mixtures in which photons emitted interact with multiple phases and can therefore result in reduced accuracy of individual mineral phase abundance estimates.

Future Work: Further development will continue to place better constraints on the uncertainties and overall mixing linearity of sedimentary rocks. This work will be enhanced in a number of ways, including: adding more clay endmembers to the spectral library, examining microRaman classes at an increased magnification, and continually expanding the amount of natural samples examined with cross analytical approaches.

References: [1] Malin and Edgett (2000), Science, v. 290, p. 1927-1937. [2] McLennan et al., (2014), Science, v. 343, p. 1244734 1-10. [3] Ruff et al., (1997), JGR, v. 102, p. 14899-14913. [4] Christensen et al., (2001), JGR, v. 105, p. 9735-9739. [5] Ramsey and Christensen (1998), JGR, v. 103, p. 577-596. [6] Feely and Christensen (1999), JGR , v. 104, p. 24195-24210. [7] Hamilton and Christensen (2000), JGR, v. 105, p. 9717-9733. [8] Wyatt et al., (2001), JGR, v. 106, p. 14711-14732. [9] Michalski et al., (2004), JGR, v. 109, p. E03007 1-15. [10] Baldridge et al., (2004), JGR, v. 109, p. E12006 1-18. [11] Michalski et al., (2006), JGR, v. 111, p. E03004 1-14. [12] Rogers and Aharonson (2008), JGR, v. 113, p. E06S14 1-19.

Acknowledgements: This work was funded by NASA MFR NNX09AL22G